ORIGINAL PAPER

Preparation of a filter bed coupled with Mn-TiO_2/ZnO nanocomposite for the treatment of micro-pollutants in municipal wastewater

Midhun Gopi[1,2], Shivaraju Harikaranahalli Puttaiah[1,2,✉]

1. Department of Water and Health, JSS Academy of Higher Education and Research, Mysuru, India-570015
2. Center for Water, Food and Energy, The GREENS trust, Harikaranahalli, Dombaranahalli Post, Turuvekere Taluka, Tumkur District, Karnataka, India-572215

Date of submission: 19 Mar 2018, ***Date of acceptance:*** 03 Jul 2019

ABSTRACT

Technical advancement is urgently required for the degradation of micro-pollutants in municipal wastewater. The present study aimed to describe the preparation of a filter-bed Mn-TiO_2/ZnO nanocomposite and degradation of micro-pollutants in real-time municipal wastewater obtained from Kesare wastewater treatment plant in Mysore district, India. Activated carbon and sand were used for the preparation of the filter bed, and activated carbon was prepared using agricultural wastes (coconut shells). Meanwhile, the visible light-responsive Mn-TiO_2/ZnO composite was prepared using the mild sol-gel technique. The composites were characterized by scanning electron microscopy, Fourier-transform infrared spectroscopy, X-ray diffraction, and photocatalytic techniques. High crystallinity, considerable shift in the band gap energy, and adequate photocatalytic activity under the visible light range were observed. In addition, the filter bed coupled with the Mn-TiO_2/ZnO nanocomposite functioned efficiently in the degradation of the common pollutants under LED irradiation as the driving source of energy.

Keywords: Sol-gel, Composite, Sewage, Filter bed, Photocatalysis, Adsorption

Introduction

Semiconductor photocatalysis is a promising technology for wastewater treatment, which is associated with the production of no residues and secondary pollutants. In general, photocatalysis is defined as the process of generating minerals through the degradation of simple organic compounds in water and air in the presence of a catalyst. Titanium dioxide (TiO_2) has been widely used in wastewater purification technologies owing to properties such as strong oxidization power, cost-efficiency, and long-term stability against photochemical corrosion.[1-4] Meanwhile, zinc oxide (ZnO) is considered beneficial for similar purposes with its unique optical and electrical properties[5] and similarity to the physicochemical properties of TiO_2.[6, 7] The band gap of TiO_2 and ZnO is 3.2 and 3.37 eV, respectively, which limits their application since they could only be active under ultraviolet (UV) light irradiation.[8, 9] Therefore, several methods have been proposed to shift the optical sensitivity of TiO_2 and ZnO from UV to the visible-light range for the efficient use of solar energy; some of these methods include element doping, metal deposition, surface sensitization, and the coupling of composite semiconductors.[10-14] In addition, it is possible to enhance the activity of TiO_2 photocatalysts through ZnO coupling.[15] Among various coupled semiconductor composites, several studies have been focused on the integration of TiO_2 with other metal oxides, such as ZnO,[16] SnO_2,[17] Fe_2O_3,[18] ZrO_2,[19] Cu_2O,[20] WO_3,[21] SiO_2,[22] and MoO_3.[23] Moreover, it has been reported that TiO_2/ZnO nanocomposites have potent physical and chemical interactions with adsorbed species, as well as a variety of applications in gas sensing materials, thermoelectric materials, dye-sensitized solar cells, piezoelectric devices, and semiconductor photocatalysts.[16, 24, 25]

Several approaches have been developed for the production of TiO_2/ZnO composites using various precursors of titania and zinc; such examples are sol-gel, solvo/hydrothermal, and co-precipitation techniques. The structure and physiochemical properties of TiO_2/ZnO composites could be affected by changes in the

✉ *Shivaraju Harikaranahalli Puttaiah*
shivarajuenvi@gmail.com

Citation: Gopi M, Shivaraju HP. Preparation of a filter bed coupled with Mn-TiO_2/ZnO nanocomposite for the treatment of micro-pollutants in municipal wastewater. J Adv Environ Health Res 2019; 7(3): 187-196

temperature, calcination process, pH, stirring speed, water-to-precursor ratio, and reagent concentration. Depending on their size, shape, and crystallographic structure, TiO_2/ZnO systems exhibit variable physiochemical properties.[26] Moreover, ZnO has a slightly more negative band gap energy compared to TiO_2, which contributes to the injection of electrons from the conduction band of ZnO to TiO_2, favoring electron-hole separation.[27] Therefore, the incorporation of these materials into a combined structure is of utmost importance considering that the resultant products may possess improved physiochemical properties. In a study in this regard, Abdel Aal *et al.* prepared TiO_2/ZnO nanopowders with various TiO_2/ZnO ratios using the hydrothermal method for the photocatalytic degradation of 2-chlorophenol. The obtained results indicated the increased degradation efficacy of the TiO_2/ZnO composite with the ratio of 90:10.[28] In another study, ZnO nanoparticles were coated on titania nanotubes (TNT) and assessed in terms of the photocatalytic degradation of rhodamine B under UV irradiation. The findings clearly demonstrated that the ZnO-TNT nanocomposite exhibited superior degradation efficacy over pure TNTs, P25, and ZnO.[29] On the other hand, Liao *et al.* investigated the photocatalytic degradation of methyl orange using TiO_2/ZnO composite nanoparticles, reporting that the TiO_2/ZnO composite nanoparticles exhibited more prominent photoactivity compared to pure TiO_2.[16]

The present study aimed to describe the preparation of a filter bed coupled with a Mn-TiO_2/ZnO nanocomposite and evaluate its application in the degradation of micro-pollutants in real-time municipal wastewater within the visible range. Filtration was employed as the preliminary treatment for the removal of the suspended particles in sewage so as to enhance light penetration.

Materials and Methods

Synthesis of photocatalytic nanocomposites

The photocatalytic Mn-TiO_2/ZnO nano-composite was prepared using the mild sol-gel technique, with TiO_2 and ZnO as the precursors. During the preparation of the Mn-TiO_2/ZnO nanocomposite, TiO_2 was added to NaOH (1 M) with constant stirring on a magnetic stirrer. Following that, approximately 0.1 mg of $MnSO_4$ was dissolved in double-distilled water and added to the homogenous mixture drop-wise as a source of Mn dopant, forming solution A. Afterwards, ZnO was dissolved in NaOH to form solution B, which was slowly added to solution A under magnetic stirring (300-450 rpm) for 12 h at room temperature, followed by aging in darkness for 24 h. At the next stage, the aqueous mixture was washed repeatedly with deionized water and dried in a dust-free hot air oven at the temperature of 50 °C. The obtained powder was treated in a dust-free muffle furnace using a silica vessel provided with a lid at the temperature of 450 °C for 2 h. Finally, it was quickly quenched to the room temperature using a cooling system in order to obtain the desired crystallinity and active surface morphology. Fig. 1 illustrates the schematic preparation of the Mn-TiO_2/ZnO nanocomposite using the mild sol-gel technique.

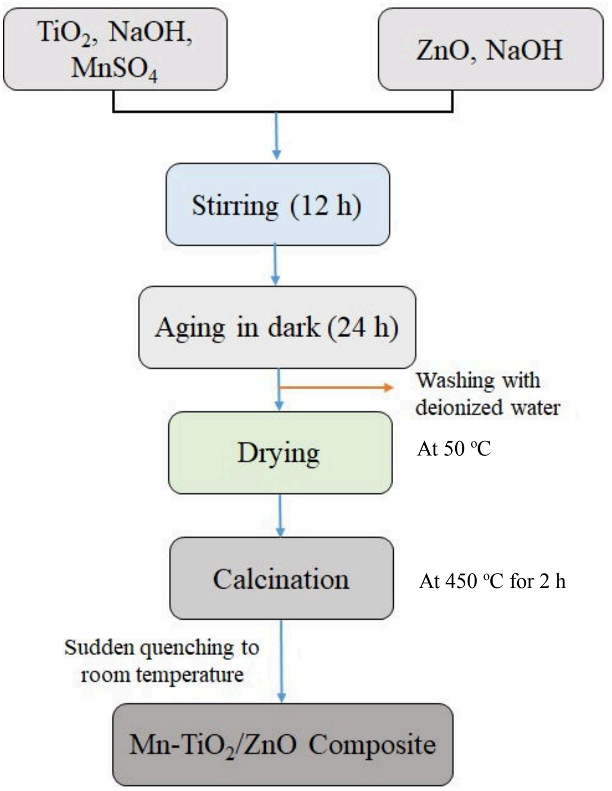

Fig. 1. Schematic of Mn-TiO_2/ZnO composite preparation through sol-gel process

Preparation of the filter bed

At this stage, a standard glass column with the length of 70 cm and diameters of 5.3 cm was used for the preparation of the filter bed. The column was fixed in a vertical position using wall clamps. The filter bed was composed of sand and activated carbon, which were added in the same order at the ratio of 2:1. The sand was collected from the nearby water bodies, washed carefully using deionized water, and dried at room temperature. In addition, the activated carbon was prepared from coconut shells under controlled conditions. In order to ensure proper filtration, the flow rate was fixed at 0.0947 m^3/s. Fig. 2 depicts the schematic representation of the filter bed.

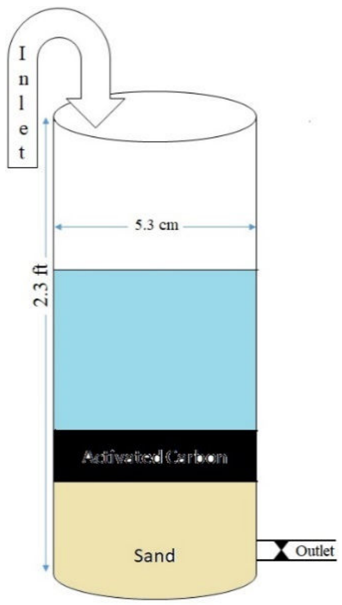

Fig. 2. Schematic of filter bed

Characterization of the nanocomposites

The prepared Mn-TiO_2/ZnO nanocomposite was characterized using various analytical techniques in order to recognize its properties. The optical and band gap energy shifting characteristics of the Mn-TiO_2/ZnO composite were investigated using a UV-visible spectrophotometer (Shimazdu UV-2100), and diluted alcohol was used for the suspension of the particles. Additionally, a powder X-ray diffractometer (Hitachi; model: S- 4000, Japan) was utilized to identify the phase composition and crystalline structures within the Bragg's angle range of 10-70^0 at the rate of 3^0 per minute using a nickel-filtered CuKa radiation source. The obtained results were ratified through the comparison of the JCPDS files (PCPDF Win-2.01).

The structural elucidation and important functional groups in the Mn-TiO_2/ZnO nanocomposite were investigated using Fourier-transform infrared spectroscopy (FTRI; JASCO-460 PLUS, Japan). The morphology and microstructures of the Mn-TiO_2/ZnO nanocomposite were scanned via scanning electron microscopy (SEM; Hitachi; model: S-4000, Japan), and the photocatalytic activity of the Mn-TiO_2/ZnO nanocomposite was determined with visible light illumination (100 W tungsten bulb, Philips) using methylene blue as the model dye solution.[2]

Filtration experiment

The filtration of the collected real-time municipal wastewater was performed using a filter bed composed of sand and activated carbon. The municipal wastewater was collected from Kesare wastewater treatment plant ($12^0$21'02.8" N $76^0$39'51.3" E), located at Kesare village in Mysore district (India). During the experiment, a specific volume of the collected wastewater was passed through a glass column with a fixed flow rate (0.0947 m^3/s). Retrospective methods were applied to determine the degradation of the micro-pollutants, as well as nitrate, nitrite, phosphate, chemical oxygen demand (COD), suspended solids, and dissolved solids.[30] The treatment efficacy (%) of the filter bed in the degradation of the municipal wastewater was calculated using Eq. 1, as follows:

$$\text{Treatment efficacy} = [(C_0 - C_i) / C_0] \times 100 \quad (1)$$

where C_0 and C_i represent the initial and final concentrations, respectively.

Photocatalytic degradation experiment

The photocatalytic degradation efficacy of the Mn-TiO_2/ZnO nanocomposite was assessed using methylene blue as the model dye with visible light illumination (100 W tungsten bulb, Philips), and the dye solution (0.01 M) was prepared using deionized water. During the photocatalytic degradation experiments, 50 mL of the dye solution was placed in a reaction vessel with the capacity of 100 mL, and 0.5 mg of the Mn-TiO_2/ZnO composite was added and exposed to the irradiation source. The experiments were carried out within 5 h of irradiation. Afterwards, the initial, interval, and final concentrations of the dye solution were determined using spectroscopic methods with the respective λ_{max} of the selected dye.[2] A double beam UV-Vis spectrophotometer (Shimazdu UV-2100, Japan) was used for the measurements.

The photocatalytic treatment of the real-time municipal wastewater using the Mn-TiO_2/ZnO nanocomposite was assessed using the same experimental procedures with various light sources. The photocatalytic experiment was carried out within 5 h of irradiation. The photocatalytic degradation efficacy (%) of the Mn-TiO_2/ZnO nanocomposite in the degradation of the micro-pollutants was calculated using Eq. 1.

Results and Discussion

UV-Vis spectrum

The absorption spectrum was used to determine the band gap energy of the nanomaterials and interpret their applications in photocatalysis. A nanomaterial/composite is considered to be photocatalytic only if the band gap energy of the nanomaterial/composite is comparable to the energy of the photons of ultraviolet or visible light (i.e., E_g<3.5 eV). Within the past decades, TiO_2 and ZnO have separately been recognized as photocatalysts, with the band gap energy of 3.2 and 3.7 eV, respectively.[2, 31] However, the wide band gap restricts the efficient utilization of sunlight. To overcome this disadvantage, various metals and non-metals have been introduced to reduce the band gap, with nanocomposites reported to exhibit improved properties. In the present study, the TiO_2/ZnO nanocomposite was recognized as a potential candidate for efficient photocatalysis, which was possible through the mutual transfer of the photogenerated charge carriers of the nanomaterials. To determine the band gap energy of the prepared nanocomposite, optical absorbance was observed using a double beam automated spectrophotometer (SHIMADZU, UV-1800). Fig. 3-a shows the UV-Vis absorption spectrum of the Mn-TiO_2/ZnO nanocomposite. An absorption band was observed at 503.48 nanometers, implying the absorption of photons by the composite within the visible range. Similar results have been reported by Zhang *et al.*[32] Moreover, the shifting of the absorption edge toward the visible region implied the band-tuning of the Mn-TiO_2/ZnO composite, which could be explained by the action of Zn^{2+} and Mn^{2+} acting as substitutional dopants on the surface and in the lattice of TiO_2. The direct band gap (E_g) of the samples was also determined by fitting the absorption data to the direct transition (Eq. 2.):

$$\alpha h\upsilon = E_d(h\upsilon - E_g)^{1/2} \qquad (2)$$

where α is the optical absorption coefficient, $h\upsilon$ shows the photon energy, E_g represents the direct band gap, and E_d is a constant.[33]

In the current research, the band gap of the prepared samples was measured by plotting $(\alpha h\upsilon)^2$ as a function of the photon energy and extrapolating the linear portion of the curve to the adsorption of equal to zero.[34] Fig. 3-b depicts the band gap energy of the Mn-TiO_2/ZnO nanocomposite, which was estimated at 2.4 eV.

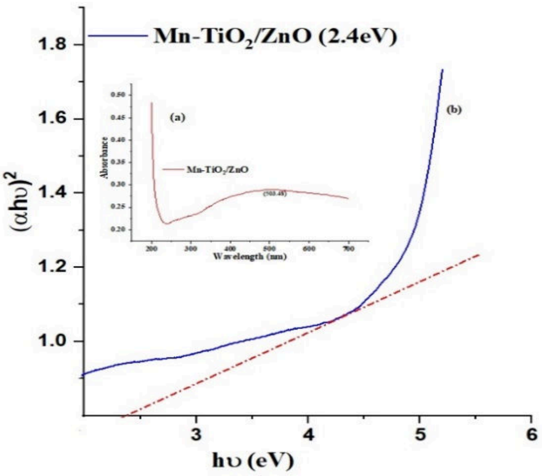

Fig. 3. Band gap energy shifting characteristics of Mn-TiO_2/ZnO nanocomposite prepared through sol-gel process

X-ray Diffraction (XRD)

In order to determine crystallinity, the prepared nanocomposite was subjected to X-ray diffraction (XRD) pattern analysis. As can be seen in Fig. 4, the peak intensities confirmed that the synthesized nanocomposite was crystalline in nature. The dominant peaks were sharp and clearly visible, particularly at 2θ of 25.3, 38.0, 48.1, and 55.1 degrees, corresponding to the (101), (004), (200), and (211) planes, respectively for anatase TiO_2 (PDF# 21-1272). Meanwhile, the peaks observed at 2ϴ of 31.7 (100), 34.34 (002), and 36.3 (101) for the ZnO were in line with the standard card PDF# 36-1451. Therefore, it could be concluded that the prepared Mn-TiO_2/ZnO nanocomposite consisted of both anatase TiO_2 and ZnO particles.

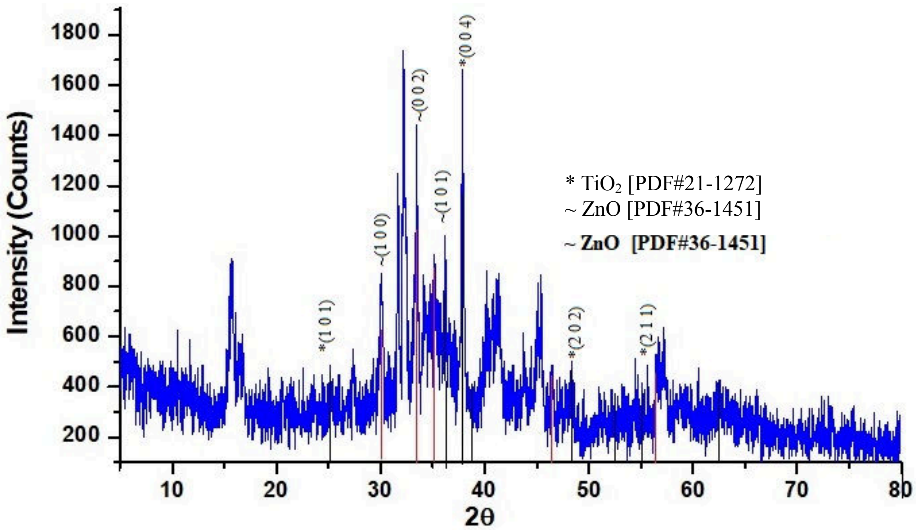

Fig. 4. Powder X-ray pattern of Mn-TiO_2/ZnO composite

FTIR

FTIR evaluations were carried out to determine the nature of the prepared nanocomposite. The obtained vibrational band is depicted in Fig. 5. In general, metal oxides exhibited the absorption band in the fingerprint region (i.e., <1,000 cm^{-1}) due to the arisen interatomic vibrations. In addition, the IR absorption band appearing within the range of 400-550 cm^{-1} was attributed to the metal-oxygen (M-O) stretching mode.[35, 36] The peaks observed at 387 cm^{-1} were the characteristic absorption peaks of the Zn-O bond, confirming the presence of ZnO. Meanwhile, the absorption peak observed at 551 cm^{-1} was ascribed to the stretching vibrations of the Ti-O-Ti groups. In addition, the IR band observed at 693 cm^{-1} was attributed to the symmetric vibration mode of the Zn-O-Ti groups.[37] These characteristic bands proved the presence of both the TiO_2 and ZnO modes in the prepared composite. On the other hand, the IR band observed within the range of 3,391-3,438 cm^{-1} was attributed to the symmetric and asymmetric stretching vibrations of the hydroxyl group (Ti-OH, Zn-OH), while the peaks identified within the range of 1,627-1,646 cm^{-1} were associated with the O-H bending vibration of the absorbed water molecules.[2, 38] The presence of the O-H bands in the spectrum was due to the physically and chemically adsorbed H_2O on the composite surface.

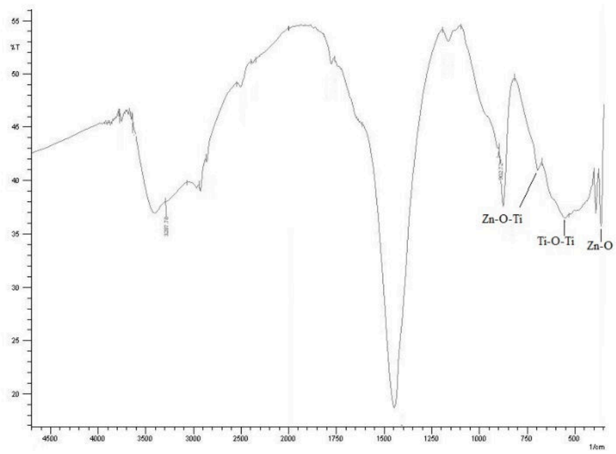

Fig. 5. FTIR spectra of Mn-TiO_2/ZnO nanocomposite

SEM

The textural features of the prepared nanocomposite were investigated using SEM. As can be seen in Fig. 6, the nanocomposite demonstrated specific morphological changes, as well as a trend of surface particle agglomeration. This is consistent with the results obtained by Katarzyna *et al.*[37] Further particles with a granular morphology are also illustrated in Fig. 6.

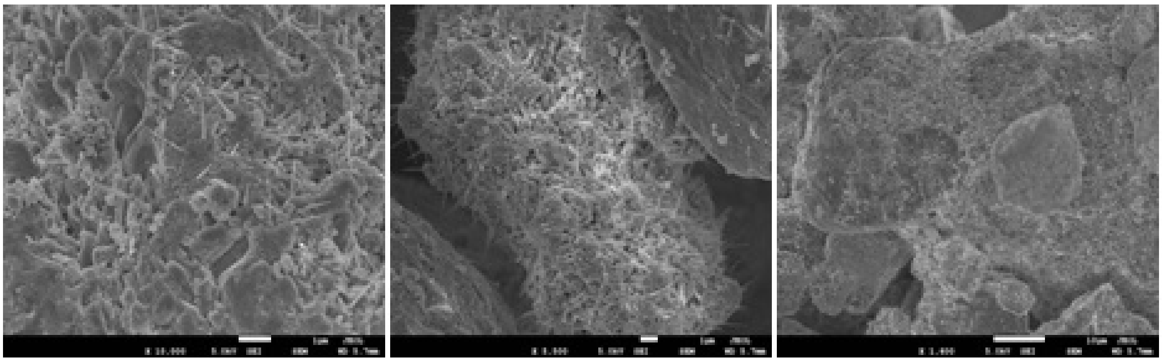

Fig. 6. SEM images of Mn-TiO_2/ZnO nanocomposite

Brunauer-Emmett-Teller (BET) surface area

The catalytic activity of the materials was determined based on several factors, such as the band gap energy and surface area. Surface area significantly influences the catalytic activity of every material. In the present study, the Brunauer-Emmett-Teller (BET) surface area of 105.6 m^2 g^{-1} was observed in the prepared composite, which was in line with the size and morphology of various nanoparticles in the TiO_2/ZnO composite. In addition, the pore volume of 0.149 cm^3 g^{-1} and pore size of 5.36 nanometers were obtained for the Mn-TiO_2/ZnO composite.[39]

Efficiency of the filter bed

Fig. 7 depicts the treatment efficacy of the filter bed utilized for the filtration of the real-time municipal wastewater collected from Kesare wastewater treatment plant located at Mysore, Karnataka (India). The initial characterization of the municipal wastewater is presented in Table 1. According to the findings, the suspended particles in wastewater inhibited the penetration of light, resulting in the hindrance of the photocatalytic process.

Therefore, the removal of the suspended solids was unavoidable prior to photocatalysis. The adsorption of the suspended particles by sand and activated carbon in the filter bed resulted in the removal of 92.2% of the suspended solids from the municipal wastewater. Furthermore, filtration was employed as a primary treatment technique for the removal of the suspended particles, which led to the degradation of micro-pollutants such as COD (88.43%), nitrate (77.03%), nitrite (40.42%), total dissolved solids (4.25%), and phosphate (3.97%) under the same experimental conditions. This could be explained by the elevated degradation efficacy of COD, nitrate, and nitrite due to the adsorption of the respective ions by activated carbon.[40-42]

In a study in this regard, Hassan and Azeema reported the possible mechanisms involved in the adsorption of ions by activated carbon. Accordingly, the adsorption sites in activated carbon could be divided into two major types, including graphene layers, which were hydrophobic in nature, and hydrophilic oxygen functional groups. As a result, the adsorption of anions occurred either by the p-orbitals of the graphene layers or through an ion exchange mechanism by the functional groups.[41-43]

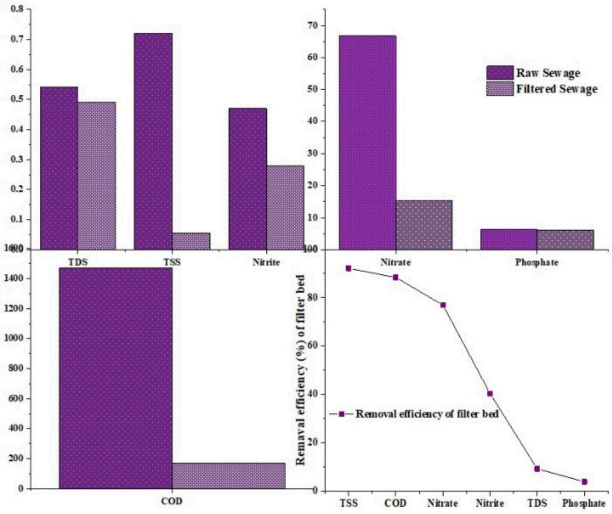

Fig. 7. Treatment efficacy of filter bed

Photocatalytic activity

The photocatalytic activity of the prepared nanocomposite was assessed using an aqueous solution of the model dye (methylene blue) with tungsten light irradiation for 4 h. Simultaneously, blank experiments were also maintained without the addition of photocatalysts (Fig. 8). The results of the blank experiments indicated that methylene blue could not be degraded without the addition of photocatalysts. Moreover, these results indicated the degradation efficacy of 86.3% with tungsten light irradiation, which was attributed to the band tuning toward the visible range, as well as the increased surface area, and increased pore size of the prepared nanocomposite.

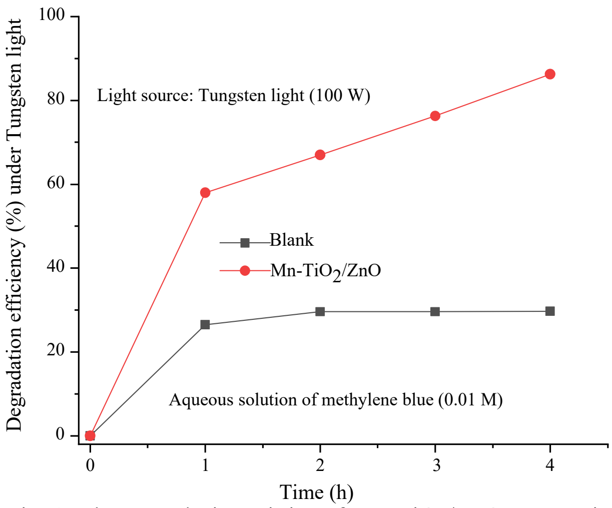

Fig. 8. Photocatalytic activity of Mn-TiO_2/ZnO composite with visible light source

Photocatalytic treatment of real-time wastewater

In the current research, the contribution of the Mn-TiO_2/ZnO nanocomposite to the photocatalytic degradation of the micro-pollutants in real-time municipal wastewater was investigated with various irradiation sources (Fig. 9).

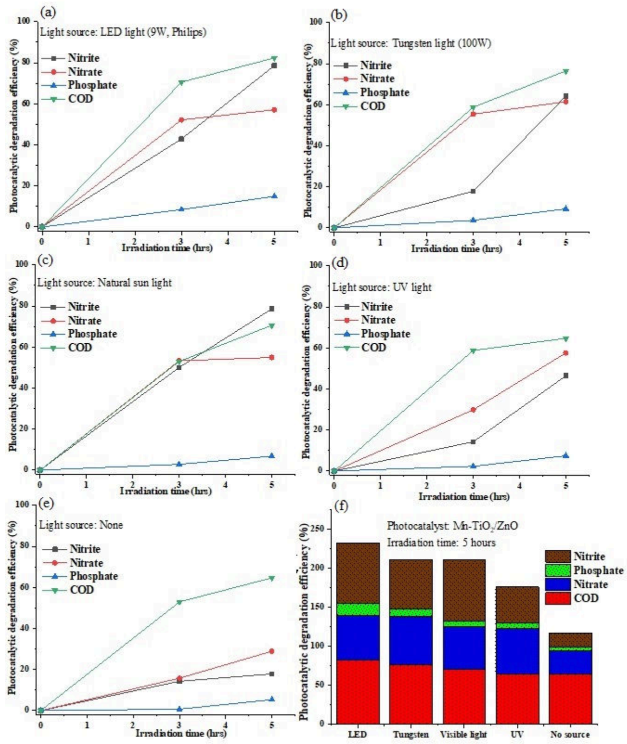

Fig. 9. Photocatalytic degradation efficacy of Mn-TiO_2/ZnO composite in degradation of micro-pollutants with various irradiation sources

In addition, the experiments were conducted in the absence of irradiation using a photocatalyst, and the obtained results clearly implied that the micro-pollutants were partially degraded in the absence of the irradiation source. This could be due to the enhanced surface area and porous structure of the composite. Moreover, the potential degradation of the pollutants was observed with the LED light source, which could be attributed to the synergistic effects of TiO_2 and ZnO in the nanocomposite with the desired properties. Therefore, it could be concluded that the co-existence of TiO_2[24] and ZnO improved the overall degradation rate of the micro-pollutants in the municipal wastewater by promoting the separation of photo-generated holes and electrons. Potential photocatalytic degradation efficacy was estimated at 82.25, 78.57, 61.4, and 14.9% for COD, nitrite, nitrate, and phosphate, respectively within 5 h of exposure to the LED light source. Such enhancement in the photocatalytic activity of the Mn-TiO_2/ZnO nanocomposite was mainly due to the presence of the ZnO/TiO_2 surface heterostructure.

Conclusion

In the current research, the Mn-TiO_2/ZnO nanocomposite was synthesized using the sol-gel technique and exhibited the band gap energy of 2.4 eV, which caused the nanocomposite to function within the visible spectrum. The XRD results confirmed the presence of TiO_2 and ZnO in the prepared nanocomposite, while FTIR confirmed the presence of both. In addition, the nanocomposite exhibited photocatalysis and adsorption, showing that the material is an effective photocatalyst. The observed adsorption process could be attributed to the increased surface area and pore size of the material. A filter bed consisting of sand and activated carbon was also employed in the primary treatment of the municipal wastewater for the removal of the suspended solids, COD, nitrate, and nitrite. The activated carbon in the filter bed could adsorb the nitrate and nitrite ions, while the sand could effectively trap the suspended solids. Therefore, it could be concluded that the employing of filtration and photocatalysis caused the micro-pollutants in real-time municipal wastewater to be degraded successfully to the safe limits prescribed by the Bureau of Indian Standards (BIS) for discharge into inland surface waters.

References

1. Shivaraju HP, Muzakkira N, Shahmoradi B. Photocatalytic treatment of oil and grease spills in wastewater using coated N-doped TiO_2 polyscales under sunlight as an alternative driving energy. Int J Environ Sci Technol 2016; 13: 2293–302.
2. Shivaraju HP, Midhun G, Anil Kumar KM, Pallavi S, Pallavi N, Shahmoradi B. Degradation of selected industrial dyes using Mg-doped TiO_2 polyscales under natural sun light as an alternative driving energy. Appl Water Sci 2017; 7: 3937–48.
3. Naldoni A, Allieta M, Santangelo S. Effect of nature and location of defects on bandgap narrowing in black TiO_2 nanoparticles. J Am Chem Soc 2012; 134(18): 7600–03.
4. Choi SK, Kim S, Lim SK, Park H. Photocatalytic comparison of TiO_2 nanoparticles and electrospun TiO_2 nanofibers: Effects of mesoporosity and interparticle charge transfer. J Phy Chem C 2010; 114(39): 16475–80.
5. Cho MH, Lee GH. Growth of high quality rutile TiO_2 thin film using ZnO buffer layer on Si(100) substrate. Thin Solid Films 2008; 516(17): 5877-80.
6. Hariharan C. Photocatalytic degradation of organic contaminants in water by ZnO nanoparticles: Revisited. Appl Catal A-Gen 2006; 304: 55-61.
7. Zhou Y, Wu WB, Hu G, Wu HT, Cui SG. Hydrothermal synthesis of ZnO nanorod arrays with the addition of polyethyleneimine. Mat Res Bull 2008; 43(8-9): 2113-8.
8. Zhou M, Yu J. Preparation and enhanced day light induced photocatalytic activity of C,N,S-tridoped titanium dioxide powders. J Hazard Mater 2008; 152(3): 1229–36.
9. Tan ST, Chen BJ, Sun X, Fan W, Kwok HS, Zhang XH, *et al.* Blueshift of optical band gap in ZnO thin films grown by metal-organic chemical-vapor deposition. J Appl phy 2005; 98(1): 013505-5.
10. Kumar SG, Devi LG. Review on modified TiO_2 photocatalysis under UV/visible light: Selected results and related mechanisms on interfacial charge carrier transfer dynamics. J Phys Chem A 2011; 115(46): 13211–41.
11. Shivaraju HP. Hydrothermal preparation of novel photocatalytic composite, TiO_2 deposited calcium alumino-silicate beads and their photocatalytic applications. Integr Publ Assoc 2011; 1(7): 1476–91.
12. Shivaraju HP, Chandrashekar CK. Photocatalytic removal of organic pollutants in silk industrial effluents by ZnO deposited CASB supported composite. Int J Res Chem Environ 2012; 2(2): 26-31.
13. Saleh R, Febiana Djaja N. Transition-metal-doped ZnO nanoparticles: Synthesis, characterization and photocatalytic activity under UV light. Spectrochimica Acta Part A: Molecular and Biomolecular Spectroscopy 2014; 130: 581-90.

14. Umaralikhan L, Jamal Mohamed Jaffar M. Green synthesis of ZnO and Mg doped ZnO nanoparticles, and its optical properties. J Mate Sci: Mater Electronics 2017; 28(11): 7677-85.
15. Chang Sung Lim. Synthesis and characterization of TiO_2-ZnO nanocomposite by a two-step chemical method. J Ceram Process Res 2010; 11(5): 631-5.
16. Liao DL, Badour CA, Liao BQ. Preparation of nanosized TiO_2/ZnO composite catalyst and its photocatalytic activity for degradation of methyl orange. J Photochem Photobiol A 2008; 194(1): 11–19.
17. Chen S, Chen L, Gao S, Cao G. The preparation of coupled SnO_2/TiO_2 photocatalyst by ball milling. Mater Chem Phys 2006; 98: 116–20.
18. Zhang XW, Lei LC. Preparation of photocatalytic Fe2O3–TiO_2 coatings in one step by metal organic chemical vapor deposition. Appl Surf Sci 2008; 254(8): 2406–12.
19. Neppolian B, Wang Q, Yamashita H, Choi H. Synthesis and characterization of ZrO_2–TiO_2 binary oxide semiconductor nanoparticles: Application and interparticle electron transfer process. Appl Catal A: Gen 2007; 333(2): 264–71.
20. Li J, Liu L, Yu Y, Tang Y, Li H, Feipeng D. Preparation of highly photocatalytic active nano-size TiO_2–Cu_2O particle composites with a novel electrochemical method. Electrochem Comm 2004; 6(9): 940–3.
21. Liu Y, Xie CS, Li J, Zou T, Zeng DW. New insights into the relationship between photocatalytic activity and photocurrent of TiO_2/WO_3 nanocomposite. Appl Catal A 2012; 433-434: 81-7.
22. Ren CJ, Qiu W, Chen YQ. Physicochemical properties and photocatalytic activity of the TiO_2/SiO_2 prepared by precipitation method. Sep Purif Technol 2013; 107: 264-72.
23. Ma BJ, Kim JS, Choi CH, Woo SI. Enhanced hydrogen generation from methanol aqueous solutions over Pt/MoO_3/TiO_2 under ultraviolet light. Int J Hydrog Energy 2013; 38: 3582–87.
24. Gui Y, Li S, Xu J, Li C. Study of TiO_2-doped ZnO thick film gas sensors enhanced by UV light at room temperature. Microeletron J 2008; 39: 1120-5.
25. Kansal SK, Singh M, Sud D. Studies on TiO_2/ZnO photocatalysed degradation of lignin. J Hazard Mater 2008; 153: 412-7.
26. Zha R, Nadimicherla R, Guo X. Ultraviolet photocatalytic degradation of methyl orange by nanostructured TiO_2/ZnO heterojunctions. J Mater Chem A 2015; 3: 6565–74.
27. Hu Z, Chen G. Novel nanocomposite hydrogels consisting of layered double hydroxide with ultrahigh tensibility and hierarchical porous structure at low inorganic content. Adv Mater 2014; 26: 5950–6.
28. Abdel Aal, Barakat MA, Mohamed RM. Electrophoreted Zn-TiO_2-ZnO nanocomposite coating films for photocatalytic degradation of 2-chlorophenol. Appl Surf Sci 2008; 254(15): 4577–83.
29. Wang LS, Xiao MW, Huang XJ, Wu YD. Synthesis, characterization, and photocatalytic activities of titanate nanotubes surface-decorated by zinc oxide nanoparticles. J Hazard Mater 2009; 161(1): 49–54.
30. Rice EW, Baird RB, Eaton AD, Clesceri LS. APHA, Standard methods for examination of water and wastewater, 22nd edn. American Public Health Association, Washington, D; 2012.
31. Norlida K, Kasim MF, Roshidah R. Band Gap narrowing and widening of ZnO nanostructures and doped materials. Nanoscale Res Lett 2015; 10: 346.
32. Zhang M, An T, Liu X, Hu X, Sheng G, Fu J. Preparation of a high-activity ZnO/TiO_2 photocatalyst via homogeneous hydrolysis method with low temperature crystallization. Mater Lett 2010; 64(17): 1883–6.
33. Gao J, Guan F, Ma Y, Yang W, Kang J, Deng H, *et al.* Preparation of CeO_2 nanoparticles and its application to ion-selective electrodes based on acetyl cellulose. Rare metals 2001; 20: 217.
34. Babitha KK, Sreedevi A, Priyanka KP, Boby S, Thomas V. Structural characterization and optical studies of CeO_2 nanoparticles synthesized by chemical precipitation. Indian J pure Appl Phy 2015; 53: 596-603.
35. Abinaya C, Marikkannan M, Manikandan M, Mayandi J, Suresh P, Shanmugaiah V, *et al.* Structural and optical characterization and efficacy of hydrothermal synthesized Cu and Ag doped zinc oxide nanoplate bactericides. Mater Chem Phy 2016; 184: 172-82.
36. Hosseini SM, Sarsari IA, Kameli P, Salamati H. Effect of Ag doping on structural, optical, and photocatalytic properties of ZnO nanoparticles. J Alloys Compd 2015; 640: 408-15.
37. Katarzyna SS, Adam K, Adam P, Joanna G, Grzegorz N, Stefan J, *et al.* TiO_2-ZnO binary

oxide systems: Comprehensive characterization and tests of photocatalytic activity. Materials 2018; 11(5): 1-19.
38. Praveen P, Viruthagiri G, Mugundan S, Shanmugam N. Sol-gel synthesis and characterization of pure and Manganese doped TiO_2 nanoparticles- a new NLO active material. Spectrochim Acta A Mol. Biomol. Spectrosc 2014; 120: 548-57.
39. Wang L, Fu X, Han Y, Chang E, Wu H, Wang H, *et al.* Preparation, characterization, and photocatalytic activity of TiO_2/ZnO nanocomposites. J Nanomater 2013; 2013: 1-6
40. Abdel-Gawad SA, Mohamed SM, Abdel Aziz HM. Adsorption study for chemical oxygen demand removal from aqueous solutions using alginate beads with entrapped activated carbon. J Indian Water Resour Soc 2017; 37(4): 8-16.
41. Hassan AH, Abdel ASM. Removal of nitrate and nitrite anions from wastewater using activated carbon derived from rice straw. J Environ Anal Toxicol 2016; 6(1): 346.
42. Lida T, Amano Y, Machida M, Imazeki F. Effect of surface property of activated carbon on adsorption of nitrate ion. Chem Pharm Bull (Tokyo) 2013; 61(11): 1173-7.
43. Giles CH, MacEwan TH, Nakhawa SN, Smith A. Studies in adsorption. Part XI. A system of classification of solution adsorption isotherms, and its use in diagnosis of adsorption mechanisms and in measurement of specific surface areas of solids. J Chem Soc 1960: 3973-93.